Food Bioscience 60 (2024) 104472

Contents lists available at ScienceDirect

Food Bioscience

journal homepage: www.elsevier.com/locate/fbio

Turning discarded blue shark (*Prionace glauca*) skin into a valuable nutraceutical resource: An enzymatic collagen hydrolysate

Ezequiel R. Coscueta [a,*], Nádia Cunha Fernandes [a], María Emilia Brassesco [a], Ana Rosa [b], André Almeida [c], Maria Manuela Pintado [a]

[a] Universidade Católica Portuguesa, CBQF - Centro de Biotecnologia e Química Fina – Laboratório Associado, Escola Superior de Biotecnologia, Rua Diogo Botelho 1327, 4169-005 Porto, Portugal
[b] SEBOL, Comércio e Indústria do Sebo, S.A., Grupo ETSA, Rua Padre Adriano nº 61, 2660-119, Santo Antão do Tojal, Portugal
[c] ITS, Indústria Transformadora de Subprodutos, S.A., Grupo ETSA, Rua da Fábrica nº 53, 2100-046, São José da Lamarosa, Portugal

ARTICLE INFO

Keywords:
Fisheries by-product
Digestive stability
Nutraceutical prototypes
Blue shark (*Prionace glauca*) skin
Antioxidant activity
Anti-inflammatory activity

ABSTRACT

Marine-derived collagen, particularly from blue shark (*Prionace glauca*) skin, represents a sustainable resource for the nutraceutical industry, yet its effective utilization remains underexplored. This study aims to optimise the enzymatic hydrolysis of blue shark skin collagen using alcalase and bromelain to enhance the bioactive properties of the resultant hydrolysates. We employed a multifactorial experimental design to determine the optimal hydrolysis conditions, assessing factors including enzyme concentration, pH, and temperature. The alcalase-treated hydrolysates demonstrated superior antioxidant and anti-inflammatory activities compared to those treated with bromelain, with increased solubilised proteins and a higher degree of hydrolysis. Notably, peptide profiles indicated that alcalase hydrolysates favoured the production of smaller peptides, suggesting enhanced bioavailability and digestive stability. *In vitro* gastrointestinal simulations demonstrated the functional stability of these peptides, indicating that while they undergo structural changes during digestion, their potential for gastrointestinal health remains significant. Our findings highlight the feasibility of converting blue shark skin, a commonly discarded by-product, into valuable nutraceutical ingredients, thus contributing to marine sustainability and waste reduction This research advances the biotechnological application of marine collagen and opens avenues for developing functional foods and pharmaceuticals.

1. Introduction

Marine-derived collagen has attracted substantial interest recently because of its distinctive characteristics and prospective uses across various industries, such as food, health, nutraceuticals, and cosmetics (Karim & Bhat, 2009; Markets and Markets, 2021). Collagen, a primary structural protein found in skin and other connective tissues, is pivotal in providing strength and structure (Bisht et al., 2021; Coscueta, Brassesco, & Pintado, 2021; Jafari et al., 2020). In the past, bovine and porcine sources have been the primary sources of collagen, but due to religious beliefs and infectious disease risks, other sources are under study (Espinales et al., 2023; Jafari et al., 2020). Marine collagen is gaining interest for its biocompatibility, environmental benefits, and lack of disease or religious concerns (Espinales et al., 2023; Jafari et al., 2020). Recent advancements in marine biotechnology have emphasized the potential of collagen hydrolysates and peptides derived from cartilaginous fish (shark, sturgeon, red stingray, skate, etc.) by-products as important bioactive compounds in nutraceutical, pharmaceutical, and cosmetic industries (Chi et al., 2014; Pan et al., 2023; Sheng et al., 2022). Studies such as those by Nikoo et al. (2022) and Costa et al. (2023) have elucidated the processes through which marine-derived collagen, particularly from aquaculture by-products, can be hydrolysed using autolytic methods to enhance their nutritional and functional properties, thereby promoting sustainable practices in marine waste utilization. Furthermore, the research highlighted by Coscueta, Brassesco, and Pintado (2021) has demonstrated that specific enzymatic treatments, such as the use of bromelain on salt-cured cod skin, can significantly enhance the antioxidant activity of collagen hydrolysates, suggesting their broader applicability in health-related sectors. These findings align with the growing interest in exploring underutilised marine resources to develop environmentally friendly and economically viable products, providing a promising avenue for our study on blue

* Corresponding author.
E-mail address: ecoscueta@ucp.pt (E.R. Coscueta).

https://doi.org/10.1016/j.fbio.2024.104472
Received 12 February 2024; Received in revised form 27 May 2024; Accepted 30 May 2024
Available online 31 May 2024

shark (*Prionace glauca*) skin collagen.

Recent advances in marine biotechnology have spotlighted the potential of enzymatically hydrolysed collagen for various applications, yet the specific utilization of blue shark skin collagen remains significantly underexplored. This study seeks to fill this gap by detailing the enzymatic hydrolysis of collagen derived from blue shark skin, a sustainable by-product of the fishing industry. While previous studies have begun to recognize the cosmetic potential of blue shark collagen (Lu et al., 2022), the broader applicability and optimal enzymatic conditions for maximizing bioactive peptide yields are not well-defined. Similarly, Rodríguez-Díaz et al. (2011) have addressed the technical optimisation of hydrolysis conditions. Nevertheless, a substantial need remains to explore how specific enzymes such as alcalase and bromelain interact with this unique collagen source to enhance its functional properties in the health, nutraceuticals, and cosmetics industries. Integrating the valorisation of discarded blue shark skin could have a relevant impact, considering the significant volumes of waste generated in the blue shark fishing industry. For example, some estimates indicate that tens of thousands of metric tonnes of blue sharks are caught yearly (Porcher & Darvell, 2022), resulting in a considerable amount of fish waste, up to 30% of which can be skin and bones (Sotelo et al., 2016). By repurposing the skin that would otherwise be thrown away or underutilised, an enormous amount of biological material can be redirected into valuable streams of bioactive compounds like collagen hydrolysates (Coscueta, Brassesco, & Pintado, 2021). Fish skin mainly comprises over 70% of collagen (Sotelo et al., 2016). This could provide fisheries with a lucrative revenue stream and significantly reduce the ecological footprint of these operations. Such a shift would be highly beneficial for marine ecosystems by reducing waste, and it would simultaneously offer new, sustainable raw materials for industries like pharmaceuticals, food, and cosmetics. Therefore, valorising blue shark skin could be a game-changer in both economic and environmental terms, harmonising industrial demands with ecological responsibility.

In enzymatic hydrolysis, alcalase and bromelain are particularly notable for their distinct catalytic capabilities and applications (Auwal et al., 2017; Coscueta, Brassesco, & Pintado, 2021; Ugwuodo et al., 2021; Vásquez et al., 2022). Alcalase, a protease derived from *Bacillus licheniformis*, is known for its broad substrate specificity and high efficiency in hydrolysing proteins into bioactive peptides, making it valuable in the food and pharmaceutical industries. Though less potent, bromelain is mainly extracted from pineapple stems and is prized in nutraceutical applications for its unique specificity (Xu et al., 2021). These enzymes have shown effectiveness across various collagen sources, including marine and freshwater fish, highlighting their potential in processing unique substrates like blue shark skin collagen (Coscueta, Brassesco, & Pintado, 2021; Jafarpour et al., 2020; Ren et al., 2008; S. Sun et al., 2022; Zamora-Sillero et al., 2018). This comparative efficiency is crucial as it informs their suitability for specific industrial uses and innovation in sustainable marine by-product use.

This research aims to delve deeply into the enzymatic hydrolysis of collagen extracted from blue shark skin, employing alcalase and bromelain to discern the optimal conditions for hydrolysis. The primary objective is to optimise hydrolysis conditions to maximize the yield and enhance the bioactive properties of the resulting collagen hydrolysates. Furthermore, this study seeks to characterise the hydrolysates' molecular size distribution and peptide profile, investigating how these properties influence the peptides' bioactivity and bioavailability. Another key aim is to assess the antioxidant and anti-inflammatory properties of the hydrolysates, including their stability and functionality throughout the digestive process. By exploring these aspects, the work intends to contribute to the sustainable use of marine by-products and to advance our understanding of marine collagen's potential, particularly from underutilised sources such as blue shark skin, thereby addressing the existing knowledge gap and suggesting practical applications in the nutraceutical industry.

2. Materials and methods

2.1. Materials and reagents

We selected blue shark (*Prionace glauca*) skin, a by-product from Brasmar - Trade Food S.A. (Guidões, Portugal) fillet processing for human consumption, as the raw material for this study. The frozen samples were ground using an industrial grinder and stored for subsequent processing. Later, ETSA - SGPS, S.A. (Empresa Transformadora de SubProdutos Animais, São José da Lamarosa, Portugal) processed all the samples under confidential industrial conditions. The skin was pretreated using sodium hydroxide sourced from VWR Chemicals via Fisher Scientific. PROZIS collagen concentrate 90 (Prozis.Com, S.A., Machico, Funchal, Portugal), with the following formulation, as described by the producer: Peptan® Hydrolysed Collagen (from fish, 143 mg/dose), chondroitin sulphate (from fish, 270 mg/dose), methylsulphonylmethane (MSM, 300 mg/dose), hyaluronic acid (143 mg/dose), anti-caking agent (magnesium salts of fatty acids), anti-caking agent (silicon dioxide). Pepsin was from porcine stomach mucosa (P7012, 500 U/mg), pancreatin from porcine pancreas (P7545, 8 trypsin U/mg), alcalase (EC 3.4.21.14), angiotensin-I-converting enzyme (ACE; EC 3.4.15.1; 5.1 U/mg), and bile salts (B863) from Sigma-Aldrich (St. Louis, MO, USA). This company provided the non-essential amino acid solution for MEM and sodium tripolyphosphate. Pineapple bromelain 1500 GDU was from AgroGrIN Tech (Porto, Portugal). Dulbecco's Modified Eagle Medium (DMEM) high glucose and the Penicillin-Streptomycin mix were from Lonza, while Biowest (Nuaillé, France) supplied the fetal bovine serum (FBS). Dialysis membranes, having a molecular pore size of 3 kDa, were procured from Spectra/Pro (Spectrum Lab, Breda, Netherlands). All other analytical grade reagents were used as received without further modification.

2.2. Multifactorial optimisation

Following the Box Behnken model, a multifactor experimental arrangement was designed to optimise hydrolysis, considering 4 factors (Table 1) and 3 responses (Table 2). Concerning the enzyme/substrate ratio, the enzyme ratio g/100 g skin (wet basis) was considered after pretreatment of non-collagenous protein extraction. In the case of bromelain, this mass was a solid product. At the same time, alcalase was liquid, which the manufacturer provided. Concerning the responses: Oxygen radical absorbance capacity (ORAC) for antioxidant capacity, the % of solubilised proteins as an efficiency indicator, and the degree of hydrolysis (DH), where the higher DH, the better enzymatic hydrolysis. A higher ORAC value highlights superior antioxidant properties essential in sectors like food and health to combat oxidative stress.

The skin pretreatment followed the methodology already applied by us (Coscueta, Brassesco, & Pintado, 2021). Shredded blue shark skin was mixed with 0.1 M NaOH at 25 °C to remove non-collagenous proteins and pigments at a sample/solution ratio of 1:10 (w/v) for 4 h at 25 °C. The mixture was centrifuged at 3857 RCF for 15 min at 4 °C. The resulting solid residue was washed with distilled water 3 times and then pH adjusted (with acid or base as needed) at 25 °C.

Each experimental design consisted of 54 individual randomised experiments. Each of the three responses considered was optimised separately and then optimised together to obtain the best conditions.

Table 1
Levels of factors evaluated on the hydrolysis process optimisation.

Factor	Alcalase		Bromelain		Units
	Low	High	Low	High	
A: pH	7	8	4	7	
B: Temperature	45	55	27	37	°C
C: Time	15	135	15	135	min
D: Ratio E/S	0.1	1.5	0.1	1.5	%

Table 2
Responses evaluated on the hydrolysis process optimisation.

Response	Units
ORAC	μmol Trolox Equivalents (TE)/g protein in the skin (DB)
Protein (BCA)	mg BSA/g protein in the skin (DB)
DH (TNBS)	%

The following joint optimal conditions were determined from optimisation (within the tested conditions) of multiple responses with Derringer's 'desirability' function.

2.3. Soluble protein content

Bicinchoninic acid (BCA) methodology (Pierce BCA Protein Assay Kit) determined the soluble protein concentration in mucus samples. Briefly, working reagent was prepared by mixing 50 parts of Reagent A with 1 part of Reagent B. Aliquots of 25 μL of each sample or protein standard were added to 200 μL of the working reagent in a 96-well microplate. The plate was then incubated at 37 °C for 30 min. Following incubation, the absorbance at 562 nm was measured using a Synergy H1 microplate reader (Biotek Instruments, Winooski, VT, USA) with Gen5 Biotek software version 3.04. Protein concentrations were calculated based on a standard curve generated using bovine serum albumin (BSA) standards.

2.4. Degree of hydrolysis

The trinitro-benzene-sulfonic acid (TNBS) method was adapted from (Hsu, 2010) for a 96-well microplate to measure the DH. Both free amine groups and those in peptide bonds were assessed using acid hydrolysis at high temperatures. Specifically, 10 mg of each freeze-dried sample was hydrolysed in 1 mL of 6 N HCl at 110 °C for 20 h. Afterwards, the hydrolysate was neutralised with 1 mL of 6 M NaOH. A ten-point L-Leucine standard curve was used, diluting a 10 mM L-Leucine solution with 0.1 M HCl. A 0.025% TNBS working solution was prepared daily by diluting a 5% commercial TNBS stock. 50 μL of the standard or sample solution was added to a 96-well microplate in duplicate, along with a blank containing 50 μL of water. Then, 125 μL of a sodium phosphate buffer (pH 8.2, 75 mM) and 50 μL of the TNBS solution were introduced to each well. The sealed microplate underwent incubation in the dark for an hour at 50 °C. The absorbance at 340 nm was read using a Synergy H1 microplate reader (Biotek Instruments, Winooski, VT, USA) with Gen5 Biotek software version 3.04. From this, the DH was calculated:

$$\mathrm{DH}\ (\%) = \frac{h_s}{h_{tot}} \times 100 \qquad \text{(Eq. 1)}$$

where h_s represents the number of amino groups (as L-leucine equivalents) of each sample and h_{tot}. The original sample contains the total number of amino groups (as L-leucine equivalents).

2.5. Antioxidant activity

2.5.1. ORAC assay

ORAC was measured using the method described by Coscueta et al. (2019). Measurements took place in a black polystyrene 96-well microplate (Nunc, Denmark) using a Multidetection plate reader (Synergy H1, Biotek Instruments, Winooski, VT, USA) operating on Gen5 Biotek software version 3.04. The fluorescence was monitored at 1 min intervals for 80 min. Each sample, standard, blank, or control analysis was performed in duplicate.

2.5.2. 2,2-Azinobis-(3-ethylbenzothiazoline-6-sulfonic acid) (ABTS) radical scavenging assay

The ABTS radical activity assesses an antioxidant's ability to neutralise the oxidised state of ABTS. The method described by Coscueta et al. (2020) was set out to measure this activity. The measurements were performed using a black polystyrene 96-well microplate (Nunc, Denmark) and a Multidetection plate reader (Synergy H1, Biotek Instruments, Winooski, VT, USA) with Gen5 Biotek software version 3.04. Before the assay, the ABTS radical absorbance to 0.70 (±0.02) was adjusted at 734 nm. A volume of 180 μL of ABTS radical were added to each 20 μL sample in the wells. Ultrapure water was used for controls alongside seven calibration solutions with Trolox (ranging from 25 to 175 μM). Each type of analysis of the sample, standard or blank, was done in duplicate.

2.6. Peptide size profile

High-Performance Size Exclusion Chromatography (HPSEC) followed the methodology described by Fernandez Cunha et al. (2023). Briefly, an Agilent AdvanceBio SEC column (Agilent Technologies, London, UK), 2.7 μm particle size, 130 Å pore size, and 7.8 inner diameter × 300 mm length was used. The column was eluted isocratically with a phosphate buffer (0.15 M NaH2PO4 pH 7) at a flow rate of 1 mL/min. The injection volume of each sample was 10 μL, and all samples were previously run through PTFE/L 0.22 μm filters. The instrument used was Waters 2690 with a photodiode array detector (PDA 190–600 nm). The software Empower 3 was used for the data collection. To determine molecular weights of the resulting chromatogram peaks, a calibration curve was made with the following protein standards: Ovalbumin (44,300 Da); Myoglobin (17,600 Da); Cytochrome C (12, 327 Da); Aprotinin (6511 Da); Neurotensin (1672 Da); Angiotensin-II (1040 Da); Tyr-Phe dipeptide (328.4 Da); and L-tryptophan (204 Da).

2.7. Functional properties

2.7.1. Foaming properties

Foaming capacity represents the volume increase due to forming a foam relative to the original volume. Foaming stability measures the foam's ability to be maintained over a certain period. The foaming properties of the pilot-scale hydrolysates were determined according to the method of Jamil et al. (2016) with slight modifications. About 10 mL of 0.5% hydrolysate solution was adjusted to pH 4, 7, and 10, followed by sonication for 10 min. The whipped sample was immediately transferred into a 25 mL measuring cylinder, and the total volume was read after 30 s (Dinakarkumar et al., 2022; Vásquez et al., 2022). The whipped sample was allowed to stand at 20 °C for 3 min, and the volume of the whipped sample was then recorded. Foaming capacity and stability were expressed as a percentage (%).

2.7.2. Emulsifying properties

The emulsifying activity index (EAI) provides insights into how emulsification evolves over a set duration, such as 10 min, and is typically measured in m^2/g. Emulsifying stability, often quantified as the emulsion stability index (ESI) in minutes, signifies the duration before phase separation begins or the resilience of the emulsion against disintegration over time. To assess the emulsifying characteristics of the pilot-scale hydrolysates, the procedure outlined by Jamil et al. (2016) was adopted, albeit with some alterations. Approximately 5 mL of vegetable oil was blended with 5 mL of a 1% hydrolysate solution at varying pH levels: 4, 7, and 10. This concoction was then sonicated. Roughly 50 μL of the resulting emulsion was sampled at the initial stage and 10 min post-sonication. Each sample was combined with 5 mL of a 0.1% sodium dodecyl sulphate (SDS) solution. The absorbance of this diluted blend was measured at 500 nm (A_{500}) right away at the start (A0) and again after 10 min (A10) of emulsion formation (Alahmad et al., 2022; Dinakarkumar et al., 2022; Hemker et al., 2020; Vásquez et al., 2022). Subsequently, the EAI and the ESI were calculated:

$$\mathrm{EAI}\ (m^2/g) = \frac{2 \times 2.303 \times A_{500}}{0.25 \times \text{sample weight}(g)} \qquad \text{(Eq. 2)}$$

$$\text{ESI (min)} = \frac{A0 \times \Delta t}{(A0 - A10)} \quad \text{(Eq. 3)}$$

where A500 is the absorbance at 500 nm, ΔA is A0 – A10 and Δt is the time at 10 min.

2.7.3. Oil-holding capacity

The oil-holding capacity (OHC) represents the amount of oil that can be held or retained by a certain amount of the substance. The OHC of the pilot-scale hydrolysates was determined using a method by Razali et al. (2015), incorporating some modifications. About 0.5 g of hydrolysate was added to 10 mL soybean oil in a 50 mL centrifuge tube and vortexed for 30 s in triplicates. The sample was thoroughly mixed and kept for 30 min at 25 °C with intermittent mixing every 10 min. Then, the content was centrifuged at 1928 RCF for 25 min at 25 °C (Alahmad et al., 2022; Dinakarkumar et al., 2022). The OHC was expressed as mL of water retained per gram hydrolysate (mL water/g hydrolysate).

2.7.4. Water-holding capacity

The water-holding capacity (WHC) indicates the amount of water that can be held or retained by a certain amount of the substance under specific conditions. The WHC of the pilot-scale hydrolysates was determined by the method described by Baharuddin et al. (2016), along with some slight modifications. Triplicate samples of 0.5 g of hydrolysate were dissolved in 10 mL of distilled water in centrifuge tubes and vortexed for 30 s. The mixture was kept at room temperature (25 °C) for 30 min and then centrifuged at 3857 RCF for 30 min at 25 °C. The supernatant was filtered with Whatman No.1 filter paper, and the volume retrieved was accurately measured (Alahmad et al., 2022; Dinakarkumar et al., 2022). Like OHC, the WHC was expressed as mL of water retained per gram hydrolysate (mL water/g hydrolysate).

2.8. Cell lines growth conditions

Human Caucasian colon carcinoma epithelial cells, Caco-2 (ECACC 86010202), were obtained from the European Collection of Authenticated Cell Cultures (Salisbury, UK). These cells were maintained in DMEM high glucose, enriched with 10% FBS, 1% penicillin-streptomycin, and MEM non-essential amino acid solution. Then, the culture was incubated at 37 °C under a humidified atmosphere of 95% air and 5% CO_2.

2.9. Metabolic inhibition on Caco-2

The cytotoxicity of the hydrolysates was tested *in vitro* on Caco-2. The cells were separated using TrypLE Express (Thermo Scientific, Waltham, MA, USA). These separated cells were seeded into 96-well Nunc Optical Btm Plt PolymerBase Black microplates at a density of 1×10^5 cells per well and were left to incubate for 24 h. After this period, the filtered culture media was replaced with sample aliquots and incubated for another 24 h. Then, the metabolic inhibition was assessed using the Presto Blue™ HS Cell Viability assay (ThermoScientific, Waltham, MA, USA) per the manufacturer's guidelines. The fluorescence was measured with a multi-detection microplate reader (Synergy H1, Biotek Instruments, Winooski, VT, USA) at excitation and emission wavelengths of 560 nm and 590 nm, respectively. The wells without cells were treated as blanks; cells in just culture media acted as controls. The metabolic inhibition was calculated:

$$\text{Metabolic inhibition (\%)} = \frac{(F_{control} - F_{sample})}{F_{control}} \times 100 \quad \text{(Eq. 4)}$$

where $F_{control}$ and F_{sample} are the fluorescence intensities (blanked data) at 590 nm of the control and sample, respectively (Coscueta, Sousa, et al., 2021).

2.10. Caco-2 immunomodulation

Based on the method described by Machado et al. (2022), Caco-2 cells were seeded in 24 well microplates at a density of 2.5×10^5 cells/well and left to incubate for 24 h. After this period, the culture media was carefully replaced with media enriched with the hydrolysates at concentrations of 15 mg/mL and 10 mg/mL, and the plates were incubated for an additional 24 h. IL-1β at 10 ng/mL was used as an inflammation control (Control+), while plain media was used as the control for basal activity (Control-). After the assay period, the supernatants were collected, centrifuged to remove debris, and stored at −80 °C for subsequent analysis. To detect Interleukin 6 (IL-6), the ELISA MAX™ Standard Set Human IL-6 (BioLegend, Inc., San Diego, CA, USA) was used according to the manufacturer's guidelines.

2.11. Gastrointestinal tract simulation

The INFOGEST protocol by Brodkorb et al. (2019) was adapted for the gastrointestinal simulation. This simulation aimed to detect changes in the size of collagen peptides during digestion and to observe any structural alterations due to enzyme activity. The procedure consisted of three stages: i) a 2 min oral phase using simulated salivary fluid (SSF) at pH 7; ii) a 120 min gastric phase with simulated gastric fluid (SGF) at pH 3; iii) a 120 min intestinal phase employing simulated intestinal fluid (SIF) at pH 7. Although this simulation incorporated digestive enzymes, it excluded amylase and lipase because the samples mainly comprise peptides. Before initiating the digestion simulation, all simulated fluids were pre-warmed to 37 °C and every sample to pH 7. Then, 1 mL of each hydrolysate or a control (distilled water) was introduced into the designated containers. The digestion began by introducing oral phase components and a 2 min vortex mixing. Subsequently, the pH was adjusted for all samples to 3 using 1 N HCl. Initiating the gastric phase, SGF, water, $CaCl_2$, and pepsin solution were added, and then the samples were shaken using an orbital shaker set at 37 °C and 130 rpm. After 2 h, the intestinal phase started by readjusting the pH value to 7 with 1 M NaOH and adding SIF, water, $CaCl_2$, and the pancreatin solution. The shaking speed was reduced to 45 rpm 500 μL aliquot was collected from each simulation stage for further analysis. To halt the reaction, these aliquots were subjected to a heat shock of 80 °C for 15 min, following the method of Brodkorb et al. (2019). The simulation of intestinal absorption was gauged by examining an aliquot sourced from within the dialysis membrane, shaken overnight using an orbital shaker set at 37 °C and 150 rpm.

2.12. Potential antihypertensive activity

The ACE inhibition (iACE) assay was followed according to Coscueta et al. (2019). Black polystyrene 96-well microplate (Nunc, Denmark) was used, and the measurement (fluorescence monitored for 80 min in intervals of 1 min) was done in a multi-detection microplate reader (Synergy H1, Biotek Instruments, Winooski, VT, USA) controlled by Gen5 Biotek software version 3.04. Every sample, blank, or control analysis was done in triplicate. The percentage of ACE activity inhibited was used to express the antihypertensive activity (Coscueta et al., 2019).

2.13. Statistics

The optimisation process yielded results that were presented as mean values and their standard deviations (SD). The responses (Y) were modelled using the following quadratic polynomial equation:

$$Y = \beta_0 + \beta_A X_A + \beta_B X_B + \beta_C X_C + \beta_D X_D + \beta_{A,A} X_A^2 + \beta_{A,B} X_A X_B + \beta_{A,C} X_A X_C + \beta_{A,D} X_A X_D + \beta_{B,B} X_B^2 + \beta_{B,C} X_B X_C + \beta_{B,D} X_B X_D + \beta_{C,C} X_C^2 + \beta_{C,D} X_C X_D + \beta_{D,D} X_D^2 + \varepsilon \quad \text{(Eq. 5)}$$

where X_A, X_B, X_C, and X_D represent the levels of the independent variables, while β_0, β_i, $\beta_{i,i}$, and $\beta_{i,j}$ denote the regression coefficients for the independent term, linear, quadratic, and binary interaction effects, respectively. The residual error is denoted as ε (Coscueta et al., 2018; Gunst, 1996). The significance of each experimental factor's effects on the response model was estimated, considering only the significant effects to derive regression models that best explained the data variability (with the best adjusted R^2). Finally, multicriteria optimisation based on Derringer's desirability function (Derringer & Suich, 1980) was applied to the experimental design results, expressing the desirability of each response value on a scale ranging from 0 to 1. The complete statistical analysis of the optimisations can be found in Annex 1.

To evaluate the antioxidant activity, ACE inhibition activity, and IL-6 release, a one-way analysis of variance (ANOVA) was applied with a confidence level set at 95.0%. The post-hoc tests were done using Tukey's Honestly Significant Difference (HSD) method to pinpoint specific distinctions between the means, maintaining the same 95.0% confidence level.

A multifactorial ANOVA was employed to study foaming and emulsifying properties, focusing on two main factors: the sample type and pH level. Again, a 95.0% confidence level was adopted. Tukey's HSD method was used in post-hoc tests to identify differences between the group means. Through this approach, we aimed to understand the combined influence of sample type and pH value on the foaming and emulsifying properties of the materials examined.

Lastly, the *t*-test was used to compare the means and contrast the oil-holding and water-holding capacities.

The primary statistical analysis was carried out using Rstudio v 2023.06.0.

3. Results

3.1. Optimisation

We explored the enzymatic hydrolysis of collagen from blue shark skin using the enzymes alcalase and bromelain to enhance its antioxidant potential by generating bioactive peptides and other valuable products.

Alcalase's final adjusted model fit well (lack of fit $P = 0.598$) and explained 75.5% of ORAC's variability (R^2). The best results for alcalase were at pH 7.3, 55.0 °C, 135 min, and an E/S ratio of 1.46, predicting an ORAC of 35.7611 μmol TE/g skin protein. In contrast, bromelain had a R^2 of 44.8%. Considering R^2 is a measure of explanatory power, not fit (lack of fit of this model $P = 0.618$), it is worth noting that a lower R^2, at this level, is not necessarily a limitation (Fig. 1A), given the intricacies of biological processes. Bromelain's optimum value was at pH 4.0, 37.0 °C, 135 min, and an E/S ratio of 1.07, forecasting an ORAC of 5.5659 μmol TE/g skin protein.

Regarding solubilised protein, alcalase's model fit well (lack of fit $P = 0.714$) and cleared up 57.8% of the variance. The optimal conditions were pH 7.8, 50.5 °C, 100 min, and an E/S ratio of 0.51, predicting 145.5 mg/g skin protein. Bromelain, with a significant fit (lack of fit $P = 0.147$) and with an R^2 of 79.9%, showed its best performance at pH 4.0, 37.0 °C, 135 min, and an E/S ratio of 0.45, anticipating 36.6 mg/g skin protein.

For DH, alcalase's model fit well (lack of fit $P = 0.959$) and covered 72.3% variance. Ideal conditions were pH 8.0, 47.3 °C, 106 min, and an E/S ratio of 0.16, projecting a DH of 15.7%. Bromelain showed low DH variability with a good fit (lack of fit $P = 0.591$) but an R^2 of 18.9%, too low to predict (Fig. 1B). This might be because, in all conditions tested, shallow values of DH were observed with practically no appreciable variation. Its optimum was at pH 4.3, 36.7 °C, 135 min, and an E/S ratio of 1.50, estimating a DH of 1.1%. Given bromelain's low R^2 for DH, we excluded it from combined optimisation.

Using the 'desirability' function, modelled in Fig. 1C, alcalase achieved peak desirability of 0.70 at pH 7.7, 51.8 °C, 103 min, and an E/S ratio of 1.46. The predicted responses were 28.098 μmol TE/g skin protein (ORAC), 145.5 mg/g skin protein, and 13.2% (DH). Bromelain's desirability (modelled in Fig. 1D) reached its optimum (1.00) at pH 4.0, 36.9 °C, 135 min, and an E/S ratio of 0.54. Predicted responses were 5.540 μmol TE/g skin protein (ORAC) and 36.3 mg/g skin protein.

In tests near optimal conditions, the skin digestion yield varied. After the whole process (pretreatment followed by hydrolysis), alcalase left 13 ± 3% of the initial skin mass (dry basis) and bromelain 35 ± 5% (dry basis). It is crucial to remember that the skin contains 75.6% moisture and 86.1% protein when dry. The pretreatment extracted non-collagenous proteins, constituting 31.2% of the skin's total protein.

3.2. Pilot-scale hydrolysis and characterisation of blue shark skin collagen hydrolysates

Considering our previously optimised conditions, ETSA tailored them to two pilot-scale processes, each corresponding to a specific enzyme. The blue shark skin collagen hydrolysates (BSCH) resultant from these processes allowed for a comprehensive assessment and characterisation of their molecular and functional properties.

3.2.1. Hydrolysates' molecular size distribution profile

We characterised the collagenous hydrolysates (BSCH with alcalase and bromelain) by their molecular size profiles. Fig. 2A displays these profiles comparatively, detailing the percentage distribution of size ranges, specifically less than 1 kDa, between 1 kDa and 3 kDa, between 3 kDa and 5 kDa, between 5 kDa and 10 kDa, between 10 kDa and 50 kDa, and greater than 50 kDa.

The results highlight how peptide fractions vary in molecular size across samples, offering insights into the composition and properties of the hydrolysates. The highest ratio for the alcalase-BSCH falls within the 3–5 kDa range (44.5%). Meanwhile, the bromelain-BSCH has its most significant ratio in the 5–10 kDa range (38.0%).

These findings highlight that the alcalase-BSCH predominantly contained smaller peptides. In contrast, bromelain-BSCH had a significant presence of larger peptides.

3.2.2. Hydrolysates' antioxidant capacity

Fig. 2B and C illustrate the antioxidant activities of the optimised hydrolysates using ORAC and ABTS assays. Alcalase-BSCH showed an ORAC value of 155 ± 14 μmol TE/g, while Bromelain-BSCH had a slightly higher ORAC of 196 ± 5 μmol TE/g, with no significant statistical difference between them ($P = 0.0572$). Conversely, the ABTS assay revealed significant differences: alcalase-BSCH recorded 109 ± 1 μmol TE/g, markedly higher than Bromelain-BSCH's 48 ± 3 μmol TE/g ($P = 0.0013$). These results suggest that alcalase hydrolysates possess stronger antioxidant activities and are potentially more effective for managing oxidative stress than bromelain hydrolysates' lower antioxidant properties.

3.2.3. Hydrolysates' foaming and emulsifying capacities and stabilities

The foaming and emulsifying properties of BSCH obtained -using both enzymes at varying pH levels were assessed. As depicted in Fig. 2D, the foaming capacity is a critical indicator of the protein's ability to reduce surface tension and stabilise air bubbles within a solution. Our analysis revealed significant differences between the enzyme treatments, with bromelain demonstrating a superior ability to maintain and stabilise foam as pH increased. Our statistical findings highlight this, which showed a pronounced variance ($P = 0.0000$) between the two treatments and across different pH levels. These results suggest that the enzymatic cleavage patterns, which possibly affect the resulting peptides' molecular size, surface hydrophobicity, and pH-induced interactions, are critical determinants of the foaming capacity (van der Ven et al., 2002). Further analysis into foam stability (Fig. 2E) reinforced these observations, with both enzyme type and pH showing significant

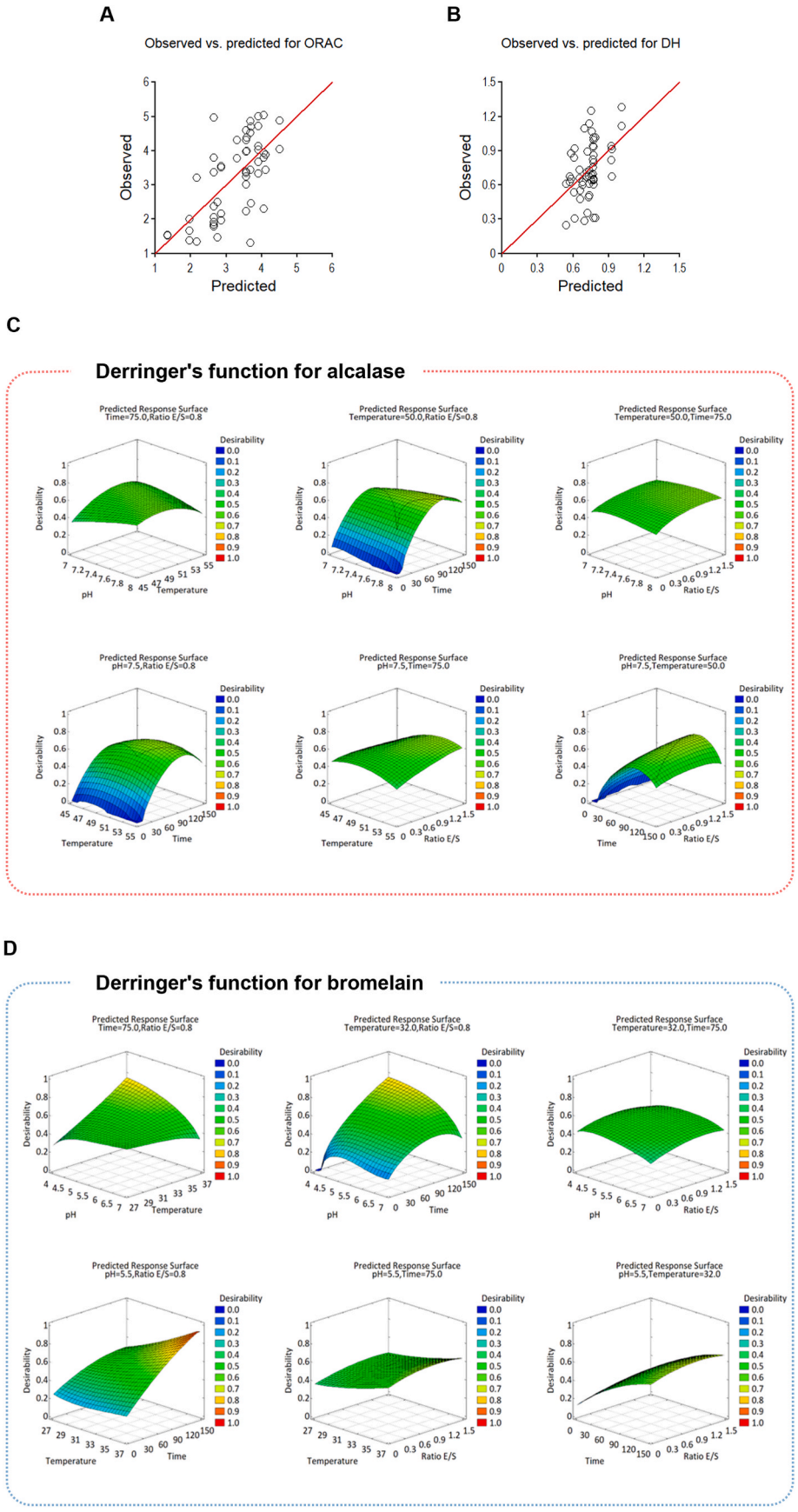

Fig. 1. Optimisation of hydrolysis using alcalase and bromelain. **A)** Observed versus predicted values for ORAC in the bromelain prediction model; **B)** observed versus predicted values for DH in the bromelain prediction model; **C)** desirability optimisation for alcalase; **D)** desirability optimisation for bromelain.

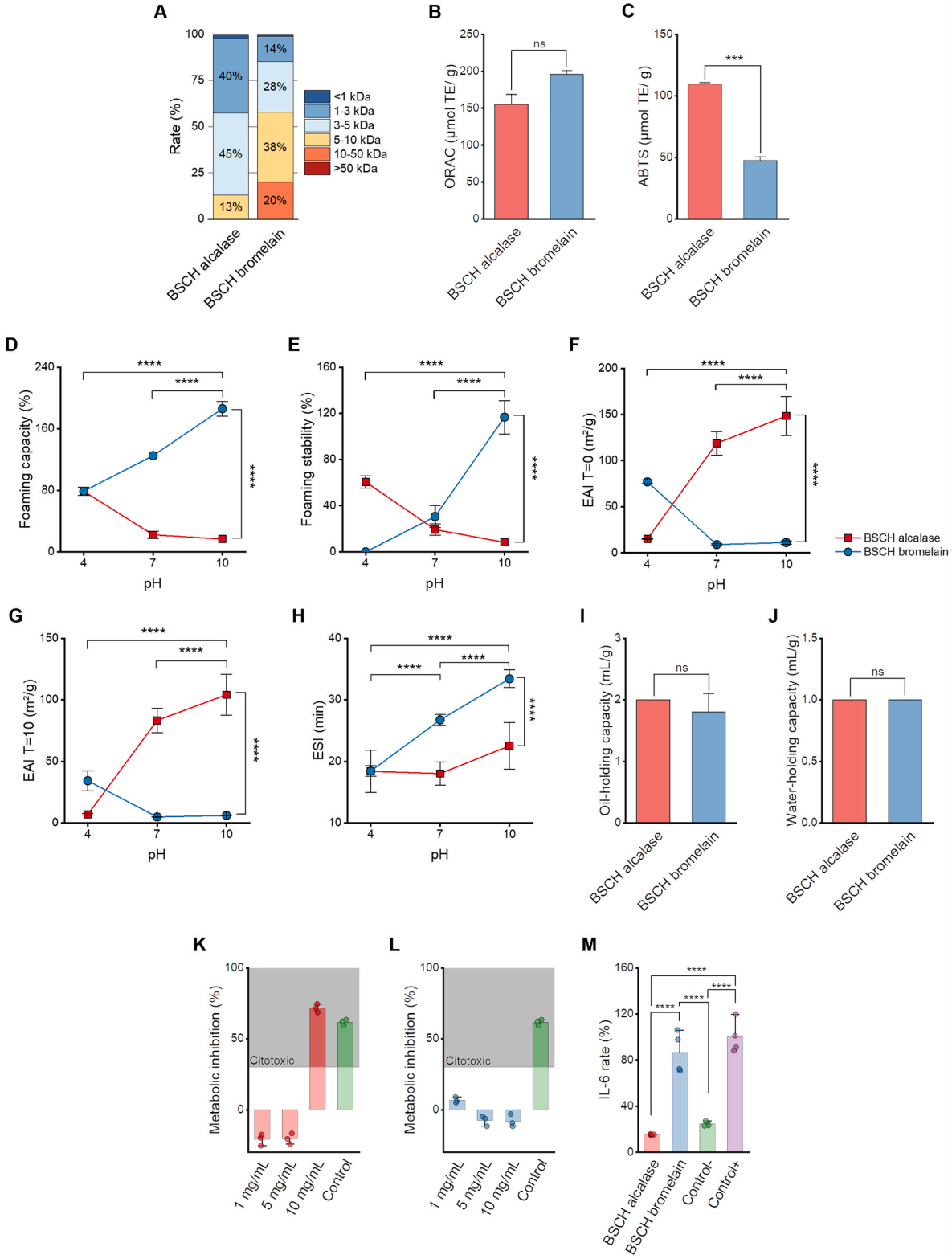

Fig. 2. Characterisation of blue shark skin collagen hydrolysates. **A)** Peptide profile rate derived from HPSEC chromatograms; **B)** antioxidant capacity assessed by ORAC; **C)** antioxidant capacity measured by ABTS; **D)** foaming capacity at pH levels 4, 7, and 10; **E)** foaming stability at pH levels 4, 7, and 10; **F)** emulsifying activity index at 0 min for pH levels 4, 7, and 10; **G)** emulsifying activity index at 10 min for pH levels 4, 7, and 10; **H)** emulsifying stability index for pH levels 4, 7, and 10; **I)** oil-holding capacity; **J)** water-holding capacity; **K)** metabolic inhibition of alcalase-BSCH at concentrations of 1, 5, and 10 mg/mL compared with a cytotoxic control (grey square indicates cytotoxic region); **L)** metabolic inhibition of bromelain-BSCH at concentrations of 1, 5, and 10 mg/mL compared with a cytotoxic control (grey square indicates cytotoxic region); **M)** immunomodulation on Caco-2 shown as a percentage rate of IL-6 release relative to the inflammation control (Control+) at a hydrolysate concentration of 5 mg/mL ns denotes $P > 0.05$; **** denotes $P \leq 0.0001$. (For interpretation of the references to color in this figure legend, the reader is referred to the Web version of this article.)

effects (P = 0.0000 for pH, P = 0.0002 for enzyme type), and their interaction also proving impactful (P = 0.0000). Notably, bromelain-BSCH displayed enhanced stability compared to those treated with alcalase, particularly at higher pH levels. This superior stability underlines bromelain's potential in applications requiring robust and enduring foam, particularly food and cosmetic products, where prolonged foam integrity is crucial. The emulsifying properties of hydrolysates at different stability phases showed clear distinctions in performance between enzyme treatments. Initially, at time zero (T = 0, Fig. 2F), both enzymes demonstrated significant influences on emulsifying activity, with enzyme type and pH displaying statistically significant effects (P = 0.0000 for enzyme type and P = 0.0008 for pH) and a significant interaction between these factors (P = 0.0000). Bromelain-BSCH exhibited superior emulsifying properties immediately after solubilization compared to alcalase, suggesting that bromelain's enzymatic action produces peptides with better surface-active properties at this initial stage.

As the test progressed to T = 10 (Fig. 2G), examining longer-term stability, the results continued to favour bromelain. Both enzyme type and pH remained significant factors (P = 0.0000 for enzyme type, P = 0.0001 for pH), with their interaction again significant (P = 0.0000). The better performance of bromelain-BSCH underscores their ability to maintain emulsion stability over time at higher pH levels, likely due to the peptides' favourable balance of hydrophilicity and hydrophobicity, which bromelain tends to produce.

Further exploration into emulsifying stability (Fig. 2H) reinforced these observations. Significant effects were again noted for enzyme type and pH (P = 0.0002 for enzyme type, P = 0.0001 for pH), with their interaction showing a notable impact, though less pronounced than in earlier tests (P = 0.0076). Bromelain's ability to consistently outperform alcalase in maintaining emulsion stability suggests that its hydrolysates are better suited for applications requiring durable and stable emulsions.

3.2.4. Hydrolysates' oil-holding and water-holding capacities

Fig. 2I and J compare the water-holding and oil-holding capacities of the optimised bromelain-BSCH and alcalase-BSCH.

The ability of hydrolysates to retain oil, termed oil-holding capacity, provides insights crucial for sectors like food processing, cosmetics, and pharmaceuticals. The bromelain-BSCH showed an oil retention value of 2.0 ± 0.0 (Fig. 2I). The alcalase-BSCH exhibited a slightly reduced capacity at 1.8 ± 0.3 (Fig. 2I). This variation in the alcalase-BSCH's performance might stem from differences in peptide sequences or the molecular makeup of the sample. Nevertheless, statistical analysis revealed no significant difference between the two samples, with a *P* of 0.373901.

On the other hand, the water-holding capacity sheds light on a hydrolysate's capability to absorb and hold water, which is vital for industries that manufacture moisture-sensitive products. Interestingly, both hydrolysates displayed a consistent water retention measure of 1.0 ± 0.0 (Fig. 2J), implying that their water interaction behaviours are similar regardless of the hydrolysing enzyme.

The statistical insignificance suggests there is no practical difference between the samples.

3.2.5. Hydrolysates' metabolic inhibition in Caco-2 cells

Fig. 2K and L displays the metabolic inhibition results (cytotoxicity) of BSCHs and control with 30% DMSO using the Caco-2 cell model (a cell line derived from human colorectal adenocarcinoma). The analytical method used was PrestoBlue.

We assessed cytotoxicity using each hydrolysate's different concentrations (1, 5, and 10 mg/mL). We express the findings as a percentage (%) of metabolic inhibition. The outcomes differ significantly across samples and concentrations. Any samples demonstrating metabolic inhibition above 30% are considered cytotoxic.

The bromelain-BSCH did not display significant cytotoxicity at any tested concentrations (Fig. 2L). However, the alcalase-BSCH exhibited high cytotoxicity with inhibitions exceeding 30% at a concentration of 10 mg/mL (72 ± 3%, Fig. 2K).

These findings suggest that different hydrolysates might have cytotoxic potential at specific concentrations. Evaluating cytotoxicity is crucial to ensure the safety of potential applications of these hydrolysates in pharmaceutical products and the development of functional foods.

It is worth noting that cytotoxicity can vary based on the concentration and the type of cells used. Therefore, future studies must clarify the action mechanisms and determine the safe concentrations for these hydrolysates.

3.2.6. Hydrolysates' immunomodulation on Caco-2 model

Fig. 2M presents the immunomodulation on Caco-2 colon cell models, measured by the percentage change in interleukin 6 (IL-6) release. The BSCHs were tested at a 5 mg/mL concentration. The inflammation was triggered by Interleukin-1-beta (IL-1-β). In scenarios with stimulation but no sample addition, the reference level was set at 100% (Control+). We identified samples with a significant decrease in IL-6 release as possessing anti-inflammatory properties. Control- represents a cell system without IL-1-β stimulation or sample addition. For analysis, we used the ELISA method.

The results indicated that IL-1-β led to a 100.0% release of IL-6, taking Control + as the reference. Conversely, Control-had a substantially lower IL-6 release at 24.7%, expected as it reflects the cell's inherent reaction in the absence of inflammatory triggers. Among the samples, alcalase-BSCH had the most significant reduction in IL-6 release, with a 15.3% compared to the Control+. This points to its promising anti-inflammatory properties. On the other hand, bromelain-BSCH had a higher IL-6 release at 86.6%, suggesting limited efficacy in reducing inflammation at the given concentration.

3.2.7. Overall implications and integrative insights

The comprehensive analysis of the functional properties of each BSCH sheds light on their multifaceted characteristics. A fundamental observation is the decisive influence of the enzyme type used in hydrolysis on the hydrolysates' molecular properties and biological effects. For instance, the differences between alcalase and bromelain treatments are evident in their antioxidant capacities, such as the ABTS antioxidant assay, and their metabolic and anti-inflammatory effects on Caco-2 cells.

While bromelain-BSCH displayed limited anti-inflammatory potential, it did not exhibit significant cytotoxicity across the tested concentrations. In contrast, alcalase-BSCH, despite its promising anti-inflammatory activity, raised safety concerns due to the cytotoxicity observed at higher concentrations (>10 mg/mL). These divergent properties highlight the intricate balance that industries must consider when harnessing the potential of these hydrolysates. Safety, particularly concerning cytotoxicity, will be paramount for any applications in pharmaceuticals or functional foods.

Furthermore, the effects of these hydrolysates are not solely determined by the enzyme type. Our findings underscore the significant interplay between enzymatic action and environmental factors, such as pH, in determining their functionalities. For instance, while enzymes primarily influenced foaming and emulsifying behaviours, pH changes altered these properties under specific conditions. This complex interaction suggests the necessity of a holistic approach when tailoring these hydrolysates for specific industrial applications.

Overall, the nuanced behaviours of BSCH, sculpted largely by enzymatic treatments, present a mosaic of challenges and opportunities for research and industry alike. It is imperative for industries seeking to capitalise on marine collagen's unique properties to understand and respect these complexities. Our findings here provide a robust foundation for future explorations and practical applications, ensuring that marine-derived collagen can be utilised to its fullest potential.

3.3. Development and in vitro digestive analysis of hydrolysate-enriched nutraceutical prototypes

A nutraceutical formulation was chosen due to the EFSA regulations on health claims for food and the growing market for hydrolysate powders and capsules as food supplements. So, a nutraceutical supplement was developed using the hydrolysate powder enriched with hyaluronic acid to reinforce the market value further. Two nutraceutical prototypes containing the two hydrolysates, alcalase-BSCH and bromelain-BSCH, were developed. Each dose comprises 900 mg of

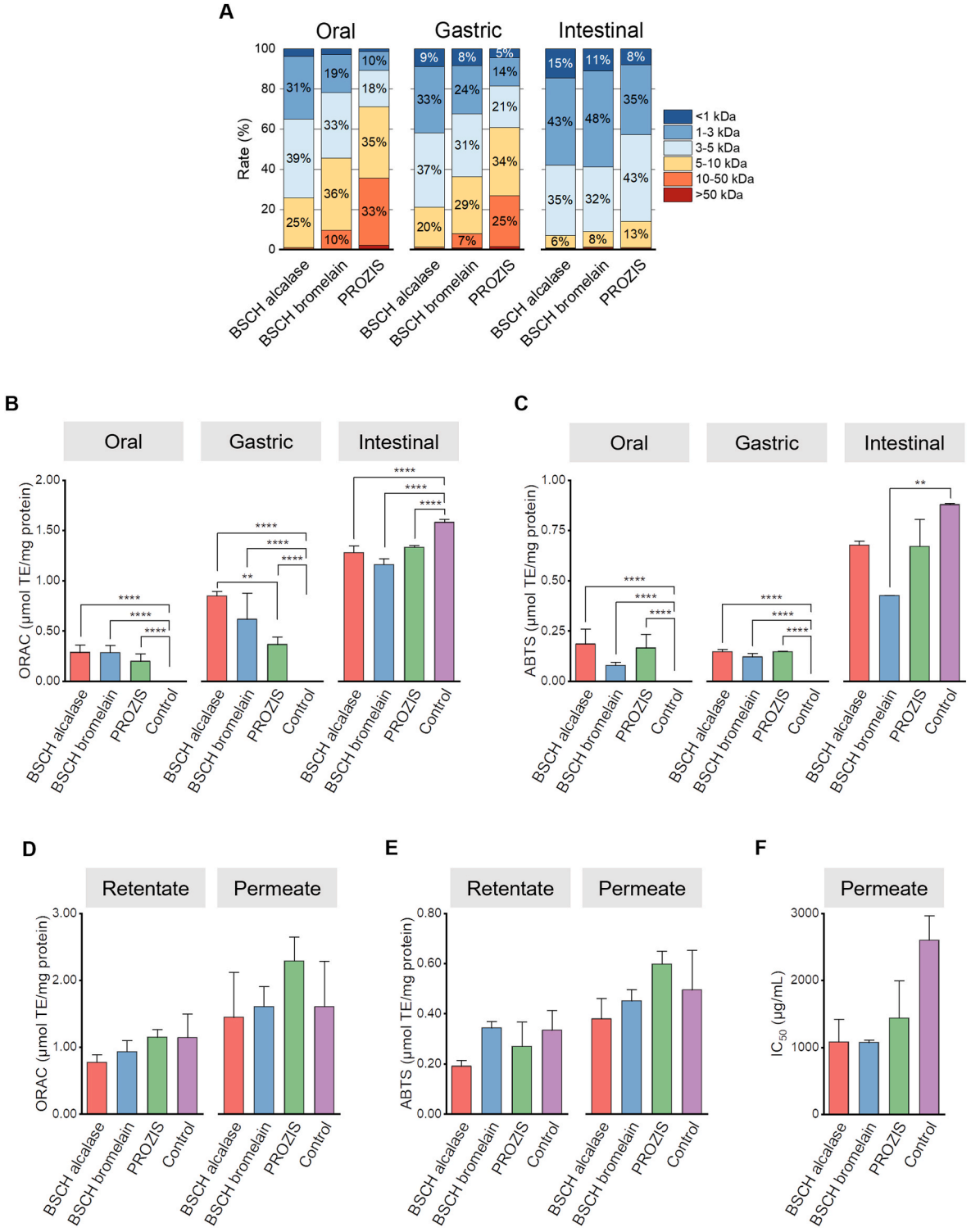

Fig. 3. *In vitro* digestion of nutraceutical prototypes. **A)** Peptide profile rate derived from HPSEC chromatograms at each digestion phase; **B)** antioxidant capacity assessed by ORAC at each digestion phase; **C)** antioxidant capacity measured by ABTS at each digestion phase; **D)** antioxidant capacity assessed by ORAC of each fraction after simulation of intestinal absorption by dialysis; **E)** antioxidant capacity assessed by ABTS of each fraction after simulation of intestinal absorption by dialysis; **F)** inhibition of ACE activity measured as IC_{50} in the permeate after simulation of intestinal absorption by dialysis. ** denotes $P \leq 0.01$; **** denotes $P \leq 0.0001$.

hydrolysate and 150 mg of hyaluronic acid. These new formulations were compared to a leading product, PROZIS' hydrolysed marine collagen supplement, which uses hydrolysates from the company Peptan®. Peptan® hydrolysate is a product described as type I collagen peptides developed explicitly for human benefit. The comparison with this benchmark helps to understand the value of the products against top market competitors.

3.3.1. *In vitro simulation of digestion*

The formulated nutraceutical prototypes were tested using a modified INFOGEST digestion simulation. The PROZIS nutraceutical product containing hydrolysed marine collagen and hyaluronic acid was used as a benchmark, and the control represents a simulation without any substrate added.

The molecular exclusion chromatography was used to study the peptide profiles (Fig. 3A). This allowed us to understand the distribution of peptide sizes in the samples during each digestion stage. During the oral phase, the digestion of peptides from PROZIS benchmark sample revealed 35% peptides in the 5–10 kDa range and 33% in the 10–50 kDa range. In contrast, the alcalase-BSCH's and bromelain-BSCH's prototypes predominantly had 3–5 kDa peptides, between 29% and 39%. Notably, the alcalase-BSCH's prototype exhibited a more significant combined percentage of peptides less than 5 kDa than the other samples.

In the gastric phase, the PROZIS sample maintained its peptides in the 5–10 kDa range at 34%. Both BSCH prototypes remained consistent, with their most significant percentages in the 3–5 kDa range, ranging from 28% to 37%. During this phase, every sample increased its percentage of peptides smaller than 1 kDa. The alcalase-BSCH and bromelain-BSCH kept their combined peptide percentages between less than 5 kDa.

During the intestinal phase, the PROZIS sample shifted its predominant peptides to the 3–5 kDa range at 43%. The other prototypes also showed the highest percentage within this range, at 32% and 37%. We noticed smaller peptides at this stage, pointing to more thorough digestion. All samples, excluding PROZIS, had a higher percentage of peptides ranging from less than 5 kDa.

These findings show that the samples responded differently during digestion. This variation likely stems from differences in their initial composition and how they react to digestive enzymes. We assessed the peptide profiles to gauge the bioavailability and potential activity of the peptides in these samples. The prototypes generally showed a higher content of smaller peptides (less than 5 kDa) than the PROZIS commercial sample at every digestion phase. This may imply that the prototypes digest more efficiently because a higher content of low-weight peptides usually suggests better digestibility.

However, it is essential to emphasise that many smaller peptides in the prototypes do not automatically suggest better bioactivity or bioavailability. A sample's peptide profile does not always directly relate to its biological function since a peptide's activity also relies on its amino acid structure and shape (Fennema et al., 2017). So, while the prototypes had smaller peptides than the PROZIS sample, we need further research to determine if this results in improved bioactivity or bioavailability.

The antioxidant activity of the prototypes was evaluated through the ORAC and ABTS tests in each phase of the gastrointestinal tract. The results presented in Fig. 3B and C demonstrated the antioxidant activity after being subjected to the oral phase of the gastrointestinal digestion simulation. In the context of antioxidant activity measured by the ORAC method, in the oral phase, the highest mean value was observed for the alcalase-BSCH's (0.288 ± 0.076 μmol TE/mg protein) and bromelain-BSCH's (0.285 ± 0.078 μmol TE/mg protein) prototypes. Both these values were statistically on par. The nutraceutical product from PROZIS showed an average of 0.199 ± 0.072 μmol TE/mg protein, and it was not significantly different from the BSCH hydrolysates in terms of antioxidant activity during the oral phase. The control, without added substrate, showed no antioxidant activity at this stage.

Regarding the antioxidant activity measured by the ABTS method in the oral phase, the alcalase-BSCH's prototype showed the highest average (0.186 ± 0.078 μmol TE/mg protein). This value was not statistically different from the PROZIS product, which had a value of 0.166 ± 0.060 μmol TE/mg protein. However, the bromelain-BSCH's prototype showed a considerably lower value of 0.079 ± 0.015 μmol TE/mg protein, which was also not statistically different.

In the gastric phase of the INFOGEST simulation protocol, antioxidant activity, measured by ORAC and ABTS techniques, showed mixed results. The control exhibited no antioxidant activity. The PROZIS benchmark displayed antioxidant activity of 0.367 ± 0.068 μmol TE/mg protein and 0.147 ± 0.003 μmol TE/mg protein for ORAC and ABTS, respectively, both statistically differentiated from the control. The bromelain-BSCH revealed antioxidant activity of 0.617 ± 0.224 μmol TE/mg protein for ORAC and 0.122 ± 0.020 μmol TE/mg protein for ABTS. These values suggested that it might not be statistically different from the PROZIS sample or the alcalase-BSCH's prototype regarding ORAC but were statistically similar regarding ABTS. Finally, the alcalase-BSCH's prototype expressed antioxidant activity of 0.850 ± 0.051 μmol TE/mg protein for ORAC, which was statistically different from the PROZIS product, and 0.147 ± 0.010 μmol TE/mg protein for ABTS.

In the intestinal phase of the INFOGEST simulation, we observed that all samples exhibited antioxidant activity. The control showcased antioxidant activity with values of 1.582 ± 0.041 μmol TE/mg protein and 0.879 ± 0.010 μmol TE/mg protein for ORAC and ABTS, respectively. The PROZIS benchmark had antioxidant activity of 1.332 ± 0.019 μmol TE/mg protein for ORAC, which was statistically different from the control, and 0.671 ± 0.138 μmol TE/mg protein for ABTS, which was not statistically different from the prototypes. The bromelain-BSCH's prototype expressed antioxidant activity of 1.162 ± 0.059 μmol TE/mg protein for ORAC and 0.427 ± 0.001 μmol TE/mg protein for ABTS. The ORAC activity for this sample was statistically similar to the other prototype. This sample showed significant differences in ABTS activity compared with all other samples. Finally, the alcalase-BSCH's prototype demonstrated an antioxidant activity of 1.281 ± 0.070 μmol TE/mg protein for ORAC and 0.678 ± 0.019 μmol TE/mg protein for ABTS. The ORAC activity was statistically aligned with the other prototype and the benchmark, while its ABTS activity showed no significant differences with the control or the benchmark.

Then, the products from the intestinal phase were subjected to a membrane dialysis process to simulate intestinal absorption. In the intestinal retention phase, all samples, including the control, showed antioxidant activity for ORAC and ABTS (Fig. 3D and E). There were no statistically significant differences between the samples for both activities. The control values were 1.143 ± 0.348 μmol TE/mg protein for ORAC and 0.335 ± 0.078 μmol TE/mg protein for ABTS. The PROZIS benchmark showed values of 1.149 ± 0.144 μmol TE/mg protein for ORAC and 0.270 ± 0.085 μmol TE/mg protein for ABTS. Bromelain-BSCH's and alcalase-BSCH's prototypes showed ORAC activities of 0.933 ± 0.149 μmol TE/mg protein and 0.776 ± 0.103 μmol TE/mg protein, and ABTS activities of 0.344 ± 0.036 μmol TE/mg protein and 0.191 ± 0.032 μmol TE/mg protein, respectively.

All samples showed antioxidant activity in the intestinal permeate phase of the INFOGEST simulation (Fig. 3D and E). In the case of ORAC activity, all samples had no statistically significant differences. The control showed an activity of 1.607 ± 0.585 μmol TE/mg protein, while the PROZIS benchmark showed an activity of 2.288 ± 0.588 μmol TE/mg protein. Bromelain-BSCH's and alcalase-BSCH's prototypes had activities of 1.607 ± 0.271 μmol TE/mg protein and 1.447 ± 0.581 μmol TE/mg protein, respectively. As for ABTS activity in the permeate, no statistical differences were observed in any of the samples. In summary, considering that the samples do not differ from the control in both permeation and retention, the idea of loss of antioxidant activity by intestinal digestion in both prototypes and benchmark is reinforced.

In addition to antioxidant activity, the ability to inhibit ACE activity, a measure of the potential for antihypertensive activity, was analysed in

the permeate. ACE inhibition was measured as IC_{50} (Fig. 3F), i.e., the 50% inhibitory concentration of the activity. Thus, higher IC_{50} values indicate lower antihypertensive activity.

In this analysis, the control showed the highest IC_{50} value of 2600 ± 516 μg/mL, indicating it has the lowest antihypertensive activity. Bromelain-BSCH's and alcalase-BSCH's prototypes presented lower IC_{50} values of 1073 ± 56 μg/mL and 1081 ± 476 μg/mL, respectively, suggesting a possible higher antihypertensive activity than the control. The PROZIS benchmark also showed an IC_{50} value of 1439 ± 784 μg/mL. However, it is essential to note that no statistically significant differences in antihypertensive activity exist between the samples.

4. Discussion

This study centred on the enzymatic hydrolysis of collagen extracted from blue shark skin using alcalase and bromelain. The aim was to determine the optimal conditions for hydrolysis and assess these enzymes' efficiency. Our primary findings revealed that collagen from blue shark skin could be efficiently processed, producing hydrolysates rich in peptides with potential bioactive properties.

In our study, alcalase exhibited higher efficiency across several parameters, including ORAC, solubilised proteins, and DH, making it a potentially more suitable enzyme for hydrolysing blue shark skin collagen. This suggests that alcalase may be more adept at breaking down collagen into bioactive peptides, possibly offering a quicker route to high-quality hydrolysates. In contrast, bromelain presented lower DH R^2 values, indicating either its specific yet less effective enzymatic action on blue shark skin collagen or a restricted range of activity. The performance of bromelain was comparatively less robust, raising questions about its commercial viability for these specific bioactivities and applications.

While earlier research has employed alcalase and bromelain on various substrates (Mazorra-Manzano et al., 2018; Real Hernandez & Gonzalez de Mejia, 2019; Zhang et al., 2013), our research offers a fresh perspective by using blue shark skin as the substrate. This approach emphasises blue shark skin's distinctiveness and potential as a valuable bio-resource. The conditions pinpointed as optimal for each enzyme align with prior literature (Coscueta, Brassesco, & Pintado, 2021; Xu et al., 2021), validating the enzymes' specificity and unique mechanisms of action. Our investigation into the peptide profile of blue shark skin unveiled distinctions from previous studies on species like tilapia and cod (Coscueta, Brassesco, & Pintado, 2021; Roslan et al., 2014; L. Sun, Hou, et al., 2017; L. Sun, Li, et al., 2017; S. Sun et al., 2022). These differences could stem from inherent contrasts between marine and freshwater fish skin or varied hydrolysis techniques.

Moreover, aligning with recent advances in biomedicine, Gao et al. (2022) explored the role of marine collagen peptides in healing oral mucosal ulcers, highlighting their regenerative potential and applicability in medical biomaterials. Complementarily, Popov et al. (2013) examined the biological activities of collagen peptides from Far-Eastern holothurians, noting varied bioactivities based on the enzyme used. These observations support our findings with bromelain's varied efficiency.

Recent investigations into marine-derived collagen peptides' bioactivity have showcased their profound impact on health, mainly through their anti-inflammatory and regenerative properties. Several studies (Chen et al., 2018; Lin et al., 2021; Subhan et al., 2017; Yang et al., 2019; Yu et al., 2023) have emphasized that collagen peptides derived from marine sources not only offer potent anti-inflammatory benefits but also significantly contribute to skin health, accelerating wound healing and improving skin elasticity. These properties make marine-derived collagen peptides highly valuable for medical and cosmetic applications, underscoring their potential as a key ingredient in skin care products and therapeutic formulations to enhance skin repair and mitigate inflammatory conditions.

The unique composition of marine collagen, with its high glycine, proline, and hydroxyproline content, helps promote the stability of collagen triple helix structures, thereby enhancing the bioavailability and efficacy of these peptides in human health. Their ability to modulate key pathways involved in inflammatory responses further illustrates their potential in chronic disease management, providing a natural alternative to synthetic drugs.

Our research on blue shark skin collagen hydrolysis parallels novel insights into marine-derived peptides' roles in biomedicine. Specifically, Qiao et al. (2022) highlight the cytoprotective effects of fourteen novel ACE-inhibitory peptides from tuna processing by-products on human umbilical vein endothelial cells, emphasizing the peptides' therapeutic potential in cardiovascular disease contexts. Additionally, Wu et al. (2023) demonstrate how antioxidant peptides from monkfish swim bladders can ameliorate non-alcoholic fatty liver disease *in vitro* by regulating the AMPK/Nrf2 pathway and suppressing lipid accumulation and oxidative stress. These studies underscore the broad bioactive capabilities of marine-derived peptides, suggesting that our findings on blue shark skin collagen could similarly contribute to developing functional products with potential health benefits, particularly in anti-inflammatory and metabolic regulatory applications.

These studies support our findings and expand the understanding of collagen peptides' roles in cytotoxic and anti-inflammatory processes, providing a deeper insight into their potential applications across pharmaceutical and nutraceutical industries. This broader perspective should be considered to harness the full potential of marine-derived collagen in developing therapeutic agents and functional foods.

Our analysis of the pilot facility's blue shark skin collagen hydrolysates revealed a peptide profile that hinted at specialised antioxidant or anti-inflammatory properties inherent to blue shark skin collagen. The evident differences in characteristics, such as foaming capacity, between the enzymes might stem from their distinct cleavage patterns and resulting peptide sizes (Fennema et al., 2017). Some peptides, as profiled, could potentially influence cellular pathways, suggesting roles in cytotoxicity or anti-inflammatory processes.

Our examination of nutraceutical prototypes showed a trend during the INFOGEST simulation, where smaller peptides were favoured, typically signifying improved digestibility. During the intestinal phase of the INFOGEST simulation, every sample showed decreased antioxidant activity. This suggests that the structural stability of the peptides in both the BSCH prototypes and the PROZIS benchmark varies due to the intestinal digestion process. Although their antioxidant properties changed during digestion, implying potential peptide modifications, the prototypes demonstrated potential antihypertensive properties. Nevertheless, a thorough analysis remains essential to confirm their practical benefits.

Our study, comprehensive as it was, presented certain limitations. The inherent unpredictability of biological systems can produce diverse outcomes. The scope of our enzyme selection and pilot study sample sizes might not encapsulate the total variability of wild blue shark samples. Furthermore, while the functional study was thorough, it might have omitted some influential determinants.

This study has expanded upon the foundational work of previous research to explore the enzymatic hydrolysis of blue shark skin collagen, identifying optimal conditions that enhance the yield and bioactivity of resultant peptides. Our findings build on earlier studies, such as those by Rodríguez-Díaz et al. (2011), which laid the groundwork for technical optimisation by delving deeper into the specific actions of alcalase and bromelain. Additionally, our research contributes to the novel application areas for blue shark skin collagen, furthering the initial cosmetic focus described by Lu et al. (2022). This study advances our understanding of marine-derived collagen's potential by filling these crucial gaps. It underscores the importance of sustainable utilization of marine by-products, paving the way for future innovations in biotechnological applications of marine resources. Besides, the work also promotes valorisation of what fisheries often discard, advocating for marine conservation alongside commercial feasibility. The potential of marine-derived

collagen, especially for pharmaceutical and food sectors, is a testament to harmonising environmental responsibility with industry demands.

5. Conclusions

This study on the enzymatic hydrolysis of collagen from blue shark skin has provided crucial insights. The best conditions to enhance enzymatic hydrolysis using alcalase and bromelain were identified. Compared to past research, the work highlights the importance of enzyme specificity and their distinct action mechanisms. Notably, the results suggest significant potential for using blue shark skin collagen hydrolysates in various sectors, such as food, health, nutraceuticals, and cosmetics. The noticeable difference in skin digestion yield between alcalase and bromelain provides essential information for making commercial decisions, with alcalase appearing as the more efficient option.

Emphasizing sustainability, our study introduces an innovative way to value what some might see as waste. This work proposes a sustainable method to address marine waste issues, maximizing the use of available resources and expanding their commercial use. Our research guides the academic community and industry, showcasing the vast potential when merging marine resources with commercial needs. Our research advances the understanding of blue shark skin collagen's potential, demonstrating enhanced bioactive peptide production through tailored enzymatic processes, which opens new avenues for sustainable utilization in health-related industries.

Building upon the insights gained from this study on the enzymatic hydrolysis of collagen from blue shark skin, several avenues for subsequent research emerge that could significantly advance our understanding and utilization of marine collagen. Firstly, exploring a broader range of enzymes beyond alcalase and bromelain could uncover more efficient or specifically targeted enzymatic processes for collagen hydrolysis, potentially enhancing the peptides' yield and bioactivity. Additionally, research into the formulation of these collagen hydrolysates into various product forms, such as nutraceuticals or cosmetics, would be valuable to determine the optimal delivery methods that maximize their beneficial properties. A focus on scalability and sustainability is also critical, as developing industrial-scale processes that are economically viable and environmentally friendly is essential for the practical application of blue shark skin collagen. Lastly, the promising preliminary data on the health benefits of these hydrolysates suggest significant potential in biomedical applications, including tissue engineering and regenerative medicine, warranting further investigation into their efficacy and mechanisms in clinical settings. These research directions continue the work initiated and open new possibilities for using marine resources to enhance human health and industry applications.

Funding

This work is funded by the European Regional Development Fund (FEDER), through the Competitiveness and Internationalisation Operational Programme (POCI), within the scope of the project with reference POCI-01-0247_FEDER-49636 "FISHCOLBOOSTER: Development of fish collagen peptides in integrated system with obtaining fractions of high value for human food, aquaculture and cosmetics."

CRediT authorship contribution statement

Ezequiel R. Coscueta: Writing – review & editing, Writing – original draft, Visualization, Validation, Supervision, Methodology, Investigation, Formal analysis, Data curation, Conceptualization. **Nádia Cunha Fernandes:** Writing – original draft, Investigation, Formal analysis. **María Emilia Brassesco:** Writing – review & editing, Validation, Formal analysis. **Ana Rosa:** Writing – review & editing, Validation, Project administration. **André Almeida:** Writing – review & editing, Supervision, Project administration, Funding acquisition. **Maria Manuela Pintado:** Writing – review & editing, Supervision, Resources, Project administration, Conceptualization.

Declaration of competing interest

None.

Data availability

Data will be made available on request.

Acknowledgements

The authors would like to thank Dr. Maria João Moreira (CBQF), for her support in the functionality testing.

References

Alahmad, K., Xia, W., Jiang, Q., & Xu, Y. (2022). Effect of the degree of hydrolysis on nutritional, functional, and morphological characteristics of protein hydrolysate produced from bighead carp (*Hypophthalmichthys nobilis*) using ficin enzyme. *Foods, 11*(9), 1320. https://doi.org/10.3390/foods11091320

Auwal, S. M., Zarei, M., Abdul-Hamid, A., & Saari, N. (2017). Optimization of bromelain-aided production of angiotensin i-converting enzyme inhibitory hydrolysates from stone fish using response surface methodology. *Marine Drugs, 15*(4), 104. https://doi.org/10.3390/md15040104

Baharuddin, N. A., Halim, N. R. A., & Sarbon, N. M. (2016). Effect of degree of hydrolysis (DH) on the functional properties and angiotensin I-converting enzyme (ACE) inhibitory activity of eel (*Monopterus* sp.) protein hydrolysate. *International Food Research Journal, 23*(4), 1424–1431.

Bisht, M., Martins, M., Dias, A. C. R. V., Ventura, S. P. M., & Coutinho, J. A. P. (2021). Uncovering the potential of aqueous solutions of deep eutectic solvents on the extraction and purification of collagen type I from Atlantic codfish (*Gadus morhua*). *Green Chemistry, 23*(22), 8940–8948. https://doi.org/10.1039/D1GC01432C

Brodkorb, A., Egger, L., Alminger, M., Alvito, P., Assunção, R., Ballance, S., Bohn, T., Bourlieu-Lacanal, C., Boutrou, R., Carrière, F., Clemente, A., Corredig, M., Dupont, D., Dufour, C., Edwards, C., Golding, M., Karakaya, S., Kirkhus, B., Le Feunteun, S., … Recio, I. (2019). INFOGEST static *in vitro* simulation of gastrointestinal food digestion. *Nature Protocols, 14*(4), 991–1014. https://doi.org/10.1038/s41596-018-0119-1

Chen, Y. P., Liang, C. H., Wu, H. T., Pang, H. Y., Chen, C., Wang, G. H., & Chan, L. P. (2018). Antioxidant and anti-inflammatory capacities of collagen peptides from milkfish (*Chanos chanos*) scales. *Journal of Food Science and Technology, 55*(6), 2310–2317. https://doi.org/10.1007/S13197-018-3148-4/METRICS

Chi, C.-F., Wang, B., Li, Z.-R., Luo, H.-Y., Ding, G.-F., & Wu, C.-W. (2014). Characterization of acid-soluble collagen from the skin of hammerhead shark (*Sphyrna lewini*). *Journal of Food Biochemistry, 38*(2), 236–247. https://doi.org/10.1111/jfbc.12042

Coscueta, E. R., Brassesco, M. E., & Pintado, M. (2021). Collagen-based bioactive bromelain hydrolysate from salt-cured cod skin. *Applied Sciences, 11*(18), 8538. https://doi.org/10.3390/app11188538

Coscueta, E. R., Campos, D. A., Osório, H., Nerli, B. B., & Pintado, M. (2019). Enzymatic soy protein hydrolysis: A tool for biofunctional food ingredient production. *Food Chemistry X, 1*(100006), Article 100006. https://doi.org/10.1016/j.fochx.2019.100006

Coscueta, E. R., Pellegrini Malpiedi, L., & Nerli, B. B. (2018). Micellar systems of aliphatic alcohol ethoxylates as a sustainable alternative to extract soybean isoflavones. *Food Chemistry, 264*, 135–141. https://doi.org/10.1016/j.foodchem.2018.05.015

Coscueta, E. R., Reis, C. A., & Pintado, M. (2020). Phenylethyl isothiocyanate extracted from watercress by-products with aqueous micellar systems: Development and optimisation. *Antioxidants, 9*(8), 698. https://doi.org/10.3390/antiox9080698

Coscueta, E. R., Sousa, A. S., Reis, C. A., & Pintado, M. (2021). Chitosan-olive oil microparticles for phenylethyl isothiocyanate delivery: Optimal formulation. *PLoS One, 16*(5), Article e0248257. https://doi.org/10.1371/journal.pone.0248257

Costa, B., de, A. M. da, Porto, A. L. F., Oliveira, V. de M., & Porto, T. S. (2023). Bioactive collagen peptides: Bibliometric approach and market trends for aquatic sources. *Food Science Today, 2*(1), 1. https://doi.org/10.58951/fstoday.2023.17

Derringer, G., & Suich, R. (1980). Simultaneous optimization of several response variables. *Journal of Quality Technology, 12*(4), 214–219. https://doi.org/10.1080/00224065.1980.11980968

Dinakarkumar, Y., Krishnamoorthy, S., Margavelu, G., Ramakrishnan, G., & Chandran, M. (2022). Production and characterization of fish protein hydrolysate: Effective utilization of trawl by-catch. *Food Chemistry Advances, 1*, Article 100138. https://doi.org/10.1016/j.focha.2022.100138

Espinales, C., Romero-Peña, M., Calderón, G., Vergara, K., Cáceres, P. J., & Castillo, P. (2023). Collagen, protein hydrolysates and chitin from by-products of fish and shellfish: An overview. *Heliyon, 9*(4), Article e14937. https://doi.org/10.1016/J.HELIYON.2023.E14937

Fennema, O. R., Damodaran, S., & Parkin, K. L. (2017). *Fennema's food chemistry* (5th ed.). CRC Press. https://doi.org/10.1201/9781315372914

Fernandez Cunha, M., Coscueta, E. R., Brassesco, M. E., Marques, R., Neto, J., Almada, F., Gonçalves, D., & Pintado, M. (2023). Exploring bioactivities and peptide content of body mucus from the lusitanian toadfish *Halobatrachus didactylus*. *Molecules, 28*(18), 6458. https://doi.org/10.3390/molecules28186458

Gao, Q., Shang, Y., Zhou, W., Deng, S., & Peng, C. (2022). Marine collagen peptides: A novel biomaterial for the healing of oral mucosal ulcers. *Dental Materials Journal, 41*(6), 850–859. https://doi.org/10.4012/DMJ.2021-323

Gunst, R. F. (1996). Response surface methodology: Process and product optimization using designed experiments. *Technometrics, 38*(3), 284–286. https://doi.org/10.1080/00401706.1996.10484509

Hemker, A. K., Nguyen, L. T., Karwe, M., & Salvi, D. (2020). Effects of pressure-assisted enzymatic hydrolysis on functional and bioactive properties of tilapia (*Oreochromis niloticus*) by-product protein hydrolysates. *Lebensmittel-Wissenschaft und -Technologie, 122*, Article 109003. https://doi.org/10.1016/j.lwt.2019.109003

Hsu, K. C. (2010). Purification of antioxidative peptides prepared from enzymatic hydrolysates of tuna dark muscle by-product. *Food Chemistry, 122*(1), 42–48. https://doi.org/10.1016/J.FOODCHEM.2010.02.013

Jafari, H., Lista, A., Siekapen, M. M., Ghaffari-Bohlouli, P., Nie, L., Alimoradi, H., & Shavandi, A. (2020). Fish collagen: Extraction, characterization, and applications for biomaterials engineering. *Polymers, 12*(10), 2230. https://doi.org/10.3390/POLYM12102230, 2020, Vol. 12, Page 2230.

Jafarpour, A., Gomes, R. M., Gregersen, S., Sloth, J. J., Jacobsen, C., & Moltke Sørensen, A. D. (2020). Characterization of cod (*Gadus morhua*) frame composition and its valorization by enzymatic hydrolysis. *Journal of Food Composition and Analysis, 89*, Article 103469. https://doi.org/10.1016/J.JFCA.2020.103469

Jamil, N. H., Halim, N. R. A., & Sarbon, N. M. (2016). Optimization of enzymatic hydrolysis condition and functional properties of eel (*Monopterus* sp.) protein using response surface methodology (RSM). *International Food Research Journal, 23*(1), 1–9.

Karim, A. A., & Bhat, R. (2009). Fish gelatin: Properties, challenges, and prospects as an alternative to mammalian gelatins. *Food Hydrocolloids, 23*(3), 563–576. https://doi.org/10.1016/j.foodhyd.2008.07.002

Lin, H., Zheng, Z., Yuan, J., Zhang, C., Cao, W., & Qin, X. (2021). Collagen peptides derived from *sipunculus nudus* accelerate wound healing. *Molecules, 26*(5), 1385. https://doi.org/10.3390/molecules26051385

Lu, W.-C., Chiu, C.-S., Chan, Y.-J., Guo, T.-P., Lin, C.-C., Wang, P.-C., Lin, P.-Y., Mulio, A. T., & Li, P.-H. (2022). An *in vivo* study to evaluate the efficacy of blue shark (*Prionace glauca*) cartilage collagen as a cosmetic. *Marine Drugs, 20*(10), 633. https://doi.org/10.3390/md20100633

Machado, M., Costa, E. M., Silva, S., Rodriguez-Alcalá, L. M., Gomes, A. M., & Pintado, M. (2022). Pomegranate oil's potential as an anti-obesity ingredient. *Molecules, 27*(15), 4958. https://doi.org/10.3390/MOLECULES27154958, 2022, Vol. 27, Page 4958.

Markets and Markets. (2021). *Marine collagen market growth opportunities, development and industry overview*. https://www.marketsandmarkets.com/Market-Reports/marine-collagen-market-155534506.html.

Mazorra-Manzano, M. A., Ramírez-Suarez, J. C., & Yada, R. Y. (2018). Plant proteases for bioactive peptides release: A review. *Critical Reviews in Food Science and Nutrition, 58*(13), 2147–2163. https://doi.org/10.1080/10408398.2017.1308312

Nikoo, M., Benjakul, S., & Ahmadi Gavlighi, H. (2022). Protein hydrolysates derived from aquaculture and marine byproducts through autolytic hydrolysis. *Comprehensive Reviews in Food Science and Food Safety, 21*(6), 4872–4899. https://doi.org/10.1111/1541-4337.13060

Pan, Z., Ge, B., Wei, M., Elango, J., & Wu, W. (2023). Isolation and biochemical properties of type II collagen from blue shark (*Prionace glauca*) cartilage. *Marine Drugs, 21*(5), 260. https://doi.org/10.3390/md21050260

Popov, A., Popov, A., Artyukov, A., Krivoshapko, O., & Kozlovskaya, E. (2013). Biological activities of collagen peptides obtained by enzymic hydrolysis from Far-Eastern holothurians. *American Journal of Biomedical and Life Sciences, 1*(1), 17. https://doi.org/10.11648/j.ajbls.20130101.14

Porcher, I. F., & Darvell, B. W. (2022). Shark fishing vs. conservation: Analysis and synthesis. *Sustainability, 14*(15), 9548. https://doi.org/10.3390/su14159548

Qiao, Q.-Q., Luo, Q.-B., Suo, S.-K., Zhao, Y.-Q., Chi, C.-F., & Wang, B. (2022). Preparation, characterization, and cytoprotective effects on HUVECs of fourteen novel angiotensin-I-converting enzyme inhibitory peptides from protein hydrolysate of tuna processing by-products. *Frontiers in Nutrition, 9*, Article 868681. https://doi.org/10.3389/fnut.2022.868681

Razali, A. N., Amin, A. M., & Sarbon, N. M. (2015). Antioxidant activity and functional properties of fractionated cobia skin gelatin hydrolysate at different molecular weight. *International Food Research Journal, 22*(2), 651–660.

Real Hernandez, L. M., & Gonzalez de Mejia, E. (2019). Enzymatic production, bioactivity, and bitterness of chickpea (*Cicer arietinum*) peptides. *Comprehensive Reviews in Food Science and Food Safety, 18*(6), 1913–1946. https://doi.org/10.1111/1541-4337.12504

Ren, J., Zhao, M., Shi, J., Wang, J., Jiang, Y., Cui, C., Kakuda, Y., & Xue, S. J. (2008). Purification and identification of antioxidant peptides from grass carp muscle hydrolysates by consecutive chromatography and electrospray ionization-mass spectrometry. *Food Chemistry, 108*(2), 727–736. https://doi.org/10.1016/j.foodchem.2007.11.010

Rodríguez-Díaz, J. C., Kurozawa, L. E., Netto, F. M., & Hubinger, M. D. (2011). Optimization of the enzymatic hydrolysis of blue shark skin. *Journal of Food Science, 76*(7), C938–C949. https://doi.org/10.1111/j.1750-3841.2011.02318.x

Roslan, J., Yunos, K. F. M., Abdullah, N., & Kamal, S. M. M. (2014). Characterization of fish protein hydrolysate from tilapia (*Oreochromis niloticus*) by-product. *Agriculture and Agricultural Science Procedia, 2*, 312–319. https://doi.org/10.1016/J.AASPRO.2014.11.044

Sheng, Y., Qiu, Y.-T., Wang, Y.-M., Chi, C.-F., & Wang, B. (2022). Novel antioxidant collagen peptides of siberian sturgeon (*Acipenserbaerii*) cartilages: The preparation, characterization, and cytoprotection of H_2O_2-damaged human umbilical vein endothelial cells (HUVECs). *Marine Drugs, 20*(5), 325. https://doi.org/10.3390/md20050325

Sotelo, C. G., Comesaña, M. B., Ariza, P. R., & Pérez-Martín, R. I. (2016). Characterization of collagen from different discarded fish species of the west coast of the iberian peninsula. *Journal of Aquatic Food Product Technology, 25*(3), 388–399. https://doi.org/10.1080/10498850.2013.865283

Subhan, F., Kang, H. Y., Lim, Y., Ikram, M., Baek, S.-Y., Jin, S., Jeong, Y. H., Kwak, J. Y., & Yoon, S. (2017). Fish scale collagen peptides protect against CoCl $_2$/TNF- α -induced cytotoxicity and inflammation via inhibition of ROS, MAPK, and NF- κ B pathways in HaCaT cells. *Oxidative Medicine and Cellular Longevity*, 1–17. https://doi.org/10.1155/2017/9703609, 2017.

Sun, S., Gao, Y., Chen, J., & Liu, R. (2022). Identification and release kinetics of peptides from tilapia skin collagen during alcalase hydrolysis. *Food Chemistry, 378*, Article 132089. https://doi.org/10.1016/j.foodchem.2022.132089

Sun, L., Hou, H., Li, B., & Zhang, Y. (2017). Characterization of acid- and pepsin-soluble collagen extracted from the skin of Nile tilapia (*Oreochromis niloticus*). *International Journal of Biological Macromolecules, 99*, 8–14. https://doi.org/10.1016/j.ijbiomac.2017.02.057

Sun, L., Li, B., Song, W., Si, L., & Hou, H. (2017). Characterization of pacific cod (*Gadus macrocephalus*) skin collagen and fabrication of collagen sponge as a good biocompatible biomedical material. *Process Biochemistry, 63*, 229–235. https://doi.org/10.1016/j.procbio.2017.08.003

Ugwuodo, C. J., Nwagu, T. N. T., Ugwu, T. T., & Onwosi, C. O. (2021). Enhancement of the anti-inflammatory effect of bromelain by its immobilization on probiotic spore of *Bacillus cereus*. *Probiotics and Antimicrobial Proteins, 13*(3), 847–861. https://doi.org/10.1007/s12602-020-09714-y

van der Ven, C., Gruppen, H., de Bont, D. B. A., & Voragen, A. G. J. (2002). Correlations between biochemical characteristics and foam-forming and -stabilizing ability of whey and casein hydrolysates. *Journal of Agricultural and Food Chemistry, 50*(10), 2938–2946. https://doi.org/10.1021/jf011190f

Vásquez, P., Sepúlveda, C. T., & Zapata, J. E. (2022). Functional properties of rainbow trout (*Oncorhynchus mykiss*) viscera protein hydrolysates. *Biocatalysis and Agricultural Biotechnology, 39*, Article 102268. https://doi.org/10.1016/j.bcab.2021.102268

Wu, M.-F., Xi, Q.-H., Sheng, Y., Wang, Y.-M., Wang, W.-Y., Chi, C.-F., & Wang, B. (2023). Antioxidant peptides from monkfish swim bladders: Ameliorating NAFLD *in vitro* by suppressing lipid accumulation and oxidative stress via regulating AMPK/Nrf2 pathway. *Marine Drugs, 21*(6), 360. https://doi.org/10.3390/md21060360

Xu, X., Qiao, Y., Shi, B., & Dia, V. P. (2021). Alcalase and bromelain hydrolysis affected physicochemical and functional properties and biological activities of legume proteins. *Food Structure, 27*, Article 100178. https://doi.org/10.1016/j.foostr.2021.100178

Yang, F., Jin, S., & Tang, Y. (2019). Marine collagen peptides promote cell proliferation of NIH-3T3 fibroblasts via NF-κB signaling pathway. *Molecules, 24*(22), 4201. https://doi.org/10.3390/molecules24224201

Yu, D., Cui, S., Chen, L., Zheng, S., Zhao, D., Yin, X., Yang, F., & Chen, J. (2023). Marine-derived bioactive peptides self-assembled multifunctional materials: Antioxidant and wound healing. *Antioxidants, 12*(6), 1190. https://doi.org/10.3390/antiox12061190

Zamora-Sillero, J., Gharsallaoui, A., & Prentice, C. (2018). Peptides from fish by-product protein hydrolysates and its functional properties: An overview. *Marine Biotechnology, 20*(2), 118–130. https://doi.org/10.1007/S10126-018-9799-3/TABLES/2

Zhang, Y., Olsen, K., Grossi, A., & Otte, J. (2013). Effect of pretreatment on enzymatic hydrolysis of bovine collagen and formation of ACE-inhibitory peptides. *Food Chemistry, 141*(3), 2343–2354. https://doi.org/10.1016/J.FOODCHEM.2013.05.058